

# Enhanced activity of tungsten doped CeAlO<sub>x</sub> catalysts for the selective catalytic reduction of NO<sub>x</sub> with NH<sub>3</sub>

Peng Zhang<sup>1</sup> · Kaihui Li<sup>1</sup> · Qingduo Lei<sup>1</sup>

Received: 2 July 2015 / Accepted: 18 August 2015 / Published online: 23 August 2015  
© Akadémiai Kiadó, Budapest, Hungary 2015

**Abstract** A series of tungsten modified CeAlO<sub>x</sub> catalysts prepared by the homogeneous co-precipitation method were used for the selective catalytic reduction NO<sub>x</sub> with NH<sub>3</sub>. The activity evaluation results exhibited that the activity of CeAlO<sub>x</sub> was enhanced by the addition of tungsten, and the CeWAlO<sub>x</sub> catalyst also showed high resistance to SO<sub>2</sub> and H<sub>2</sub>O poisoning at 300 °C. The BET analysis results showed that the total pore volume and the average pore diameter of the CeAlO<sub>x</sub> catalyst was improved by the addition of WO<sub>3</sub>. The NH<sub>3</sub>-TPD, in situ DRIFTS, H<sub>2</sub>-TPR and XPS characterization results displayed that the introduction of tungsten could enhance the amount of acid sites, the adsorbability to the NH<sub>3</sub>, the redox ability and the amount of oxygen vacancies, which should be the critical factors for the CeWAlO<sub>x</sub> catalyst to achieve high NH<sub>3</sub>-SCR performance.

**Keywords** Selective catalytic reduction · NH<sub>3</sub> · Tungsten doped · Characterization

## Introduction

The emission of NO<sub>x</sub> gases produced from stationary sources has received tremendous attention because they can result in acid rain, ozone depletion, photochemical smog etc [1]. Selective catalytic reduction of NO<sub>x</sub> with NH<sub>3</sub> (NH<sub>3</sub>-SCR) is a commercially proven technology for NO<sub>x</sub> abatement produced from power plant flue gases. Commercially available catalysts are made up of the anatase TiO<sub>2</sub> carrier supporting the active components, i.e. V<sub>2</sub>O<sub>5</sub>-WO<sub>3</sub>/TiO<sub>2</sub> or V<sub>2</sub>O<sub>5</sub>-MoO<sub>3</sub>/TiO<sub>2</sub>. However, some defects still remain in this catalyst, such as the narrow operational

---

✉ Peng Zhang  
zhangpeng@ncwu.edu.cn

<sup>1</sup> School of Environmental and Municipal Engineering, North China University of Water Resources and Electric Power, Zhengzhou 450011, China

temperature window (350–400 °C), the toxicity of vanadium pentoxide to the environment and human health and poor N<sub>2</sub> selectivity in the high temperature et al. [2–4]. Therefore, many researchers are focusing on developing environmental-friendly NH<sub>3</sub>-SCR catalysts with promising performance in a broad temperature scope.

Cerium based oxide catalysts with the superiority of unique oxygen storage capacity and excellent redox properties are thought to be the substitute for the commercial catalyst. Shen et al. developed a novel CeO<sub>2</sub>/Al<sub>2</sub>O<sub>3</sub> catalyst supported on the activated-ceramics, which exhibited high activity in the temperature range from 250 to 350 °C [5]. Guo et al. investigated the relationship between the prepared method and the NH<sub>3</sub>-SCR catalytic activity for the CeO<sub>2</sub>-Al<sub>2</sub>O<sub>3</sub> catalyst [6]. However, the anti-poisoning to the SO<sub>2</sub> and the narrow reaction temperature window for the CeO<sub>2</sub>-Al<sub>2</sub>O<sub>3</sub> catalyst are thought to be the key factors restrict its further industrial application. Molybdenum modified CeAlO<sub>x</sub> catalyst was reported by Li et al. [7], which exhibited high NO conversion at a broad temperature range from 200 to 400 °C, yet the N<sub>2</sub> selectivity needed to be further improved in the high temperature. In addition, WO<sub>3</sub> has been used as a promoter to enhance the NO<sub>x</sub> conversion in the V<sub>2</sub>O<sub>5</sub>-WO<sub>3</sub>/TiO<sub>2</sub> catalyst for many years, which could strengthen acid sites on the catalyst surface. In this study, a series of tungsten doped CeAlO<sub>x</sub> catalysts were synthesized by the homogeneous co-precipitation method and used for the NH<sub>3</sub>-SCR reaction process, the corresponding substantial changes were characterized by the Brunauer–Emmett–Teller (BET), X-ray diffraction (XRD), NH<sub>3</sub>-temperature-programmed desorption (NH<sub>3</sub>-TPD), hydrogen-temperature-programmed reduction (H<sub>2</sub>-TPR), X-ray photoelectron spectroscopy (XPS) and the in situ diffuse reflectance infrared Fourier transform spectroscopy (in situ DRIFTS).

## Experimental

### Catalyst preparations

Tungsten doped CeAlO<sub>x</sub> catalysts were prepared by the homogeneous co-precipitation method using (NH<sub>4</sub>)<sub>10</sub>W<sub>12</sub>O<sub>41</sub>, Ce(NO<sub>3</sub>)<sub>3</sub>·5H<sub>2</sub>O and Al(NO<sub>3</sub>)<sub>3</sub>·9H<sub>2</sub>O as precursors. Certain amounts of (NH<sub>4</sub>)<sub>10</sub>W<sub>12</sub>O<sub>41</sub> with an equal weight of H<sub>2</sub>C<sub>2</sub>O<sub>4</sub>·2H<sub>2</sub>O were added into deionized water. After the dissolution of (NH<sub>4</sub>)<sub>10</sub>W<sub>12</sub>O<sub>41</sub>, the solution of Ce(NO<sub>3</sub>)<sub>3</sub>·5H<sub>2</sub>O and Al(NO<sub>3</sub>)<sub>3</sub>·9H<sub>2</sub>O was added with the required molar ratio. Then excess urea aqueous solution was added into the mixed solution, with the urea/(Ce + W+Al) molar ratio being 15:1, the mixed solution was then heated at 90 °C for 12 h in the water bath. The precipitated solids were collected by filtration and washed with the deionized water, followed by drying at 105 °C for 12 h and subsequently calcined at 500 °C for 5 h. Finally, the catalysts were crushed and sieved to 40–60 mesh for test purposes.

### Catalyst characterization

The specific surface area, pore volume and the average pore size of the samples were obtained by N<sub>2</sub> adsorption/desorption at 77 K by using a Micromeritics ASAP

2010 instrument. Prior to the N<sub>2</sub> adsorption, the catalysts were degassed at 90 °C for 1 h and 300 °C for 4 h. The specific surface areas of the catalysts were determined by using the BET method under the 0.05–0.3 partial pressure range. The total pore volume and the average pore diameters were measured from the N<sub>2</sub> desorption branches of the isotherms using the Barret–Joyner–Halenda (BJH) method.

The crystallinity of the catalysts were measured by means of powder XRD patterns obtained on a Rigaku D/max 2200 with Cu K<sub>α</sub> radiation, scanning between 20° and 80° at a step of 5°/min.

Hydrogen-temperature-programmed reduction (H<sub>2</sub>-TPR) and NH<sub>3</sub>-temperature programmed-desorption (NH<sub>3</sub>-TPD) profiles were measured by using a chemisorption analyzer (Micromeritics, Chemisorb 2729 TPx). For the H<sub>2</sub>-TPR, in each experiment, about 50 mg sample was loaded into the quartz reactor and pretreated in He (50 mL/min) at 300 °C for 1 h. The sample was then cooled to room temperature under flowing N<sub>2</sub>. The sample was reduced starting at room temperature and increasing up to 800 °C in a gas mixture of 10 % H<sub>2</sub>/He at 10 °C/min. The consumption of H<sub>2</sub> was monitored continuously by using a thermal conductivity detector. For the NH<sub>3</sub>-TPD experiments, after pretreatment in a He stream at 200 °C for 1 h, the catalysts were saturated with NH<sub>3</sub> at a flow rate of 40 mL/min for 1 h. Desorption was carried out by heating the catalyst in He from 100 to 600 °C with a heating rate of 10 °C/min.

The in situ DRIFTS experiments were performed on a Fourier transform infrared (FT-IR) spectrometer (Nicolet Nexus 670) equipped with an in situ diffuse reflection chamber and high sensitivity mercury–cadmium–telluride (MCT) detector cooled by liquid nitrogen. About 50 mg sample was placed in the in situ chamber. The mass flow controllers and a temperature controller were used to simulate the reaction conditions. Prior to each experiment, the catalyst was heated at 500 °C for 30 min in a flow of 10 % O<sub>2</sub>/N<sub>2</sub> and then cooled to 200 °C. The background spectrum was recorded and subtracted from the sample spectrum. All the spectra were collected with an accumulating 100 scans at a resolution of 4 cm<sup>-1</sup>.

### Catalytic activity tests

The catalytic activity tests for the selective catalytic reduction of NO with NH<sub>3</sub> were carried out in a fixed bed reactor. The simulated gas for these tests contained 1000 ppm NO, 1000 ppm NH<sub>3</sub>, 5 % O<sub>2</sub>, 8 % H<sub>2</sub>O (when used), 100 ppm SO<sub>2</sub> (when used) and balance N<sub>2</sub>. Water vapor was generated by passing N<sub>2</sub> through a heated gas-wash bottle containing deionized water. The catalytic reactions were carried out at temperatures from 100 to 400 °C under atmospheric pressure, with a total flow rate of 500 mL/min. The NO and NO<sub>2</sub> concentrations before and after reaction were determined by using a NO–NO<sub>2</sub>–NO<sub>x</sub> analyzer (Thermo, Model 42i-HL). The N<sub>2</sub>O concentration was analyzed by a gas chromatograph (Agilent 6820) with a Porapak Q column. The SCR catalytic activity and N<sub>2</sub> selectivity of the catalysts were expressed by the following equation:

$$\text{NO conversion} = ([\text{NO}_x]_{\text{in}} - [\text{NO}_x]_{\text{out}}) / [\text{NO}_x]_{\text{in}} \times 100 \%,$$

$$\text{N}_2 \text{ selectivity} = (1 - 2[\text{N}_2\text{O}]_{\text{out}} / ([\text{NO}_x]_{\text{in}} - [\text{NO}_x]_{\text{out}})) \times 100 \%,$$

with  $[\text{NO}_x] = [\text{NO}] + [\text{NO}_2]$ .

## Results and discussion

### Catalytic activity evaluation

Fig. 1 shows the NO conversion and N<sub>2</sub> selectivity over CeAlO<sub>x</sub> and W modified CeAlO<sub>x</sub> catalyst for the selective catalytic reduction of NO by NH<sub>3</sub>. Obviously, the CeAlO<sub>x</sub> catalyst showed relatively poor performance in the tested temperature range. However, the addition of W to the CeAlO<sub>x</sub> catalyst has remarkable influence on the NO conversion and N<sub>2</sub> selectivity. When the W doped molar ratio reached 1.0, more than 95 % NO conversion was attained from 225 to 400 °C and almost no N<sub>2</sub>O could be detected in the tested condition. However, further increasing the W/Al molar ratio decreased the NO conversion slightly both at low and high temperatures, although the N<sub>2</sub> selectivity showed no changes. The above results suggested that the CeWAlO<sub>x</sub> catalyst with W/Al molar ratio being 1:1 exhibited the best NH<sub>3</sub>-SCR performance.

In order to investigate the effects of SO<sub>2</sub> and H<sub>2</sub>O on the NH<sub>3</sub>-SCR performance over the W doped CeAlO<sub>x</sub> catalyst, the CeWAlO<sub>x</sub> catalyst was selected to study the influences of 100 ppm SO<sub>2</sub> or/and 8 % H<sub>2</sub>O on the performance at 300 °C and the corresponding results are illustrated in Fig. 2. It can be seen from the results that a slight decline in NO conversion occurred after the 100 ppm SO<sub>2</sub> was added, after removing SO<sub>2</sub> the NO conversion recovered immediately. When 8 % water vapor was introduced into the stream, the NO conversion was kept above 97 % during the tested period. When the 100 ppm SO<sub>2</sub> and 8 % H<sub>2</sub>O were injected into the feed gases in the meanwhile, the NO conversion decreased much more severely compared with only adding SO<sub>2</sub> or H<sub>2</sub>O. However, the conversion was still maintained at a relatively high level with more than 90 % NO conversion attained during the measured period. The above results suggested that the catalyst had better SO<sub>2</sub>/H<sub>2</sub>O durability.

### Characterization of catalysts

#### XRD

The XRD patterns of the CeAlO<sub>x</sub> and W modified CeAlO<sub>x</sub> catalysts are shown in Fig. 3. Among all the catalysts, it can be found that there were some peaks appearing at 2θ values of 28.5°, 33.2°, 47.5° and 56.5°, which can be assigned to the cerianite CeO<sub>2</sub>, yet no diffraction peaks attributed to WO<sub>3</sub> could be found, which indicated that WO<sub>3</sub> existed mainly in the amorphous state or major in highly dispersed state on the Ce–W–AlO<sub>x</sub> catalysts. In the meanwhile, no alumina phase

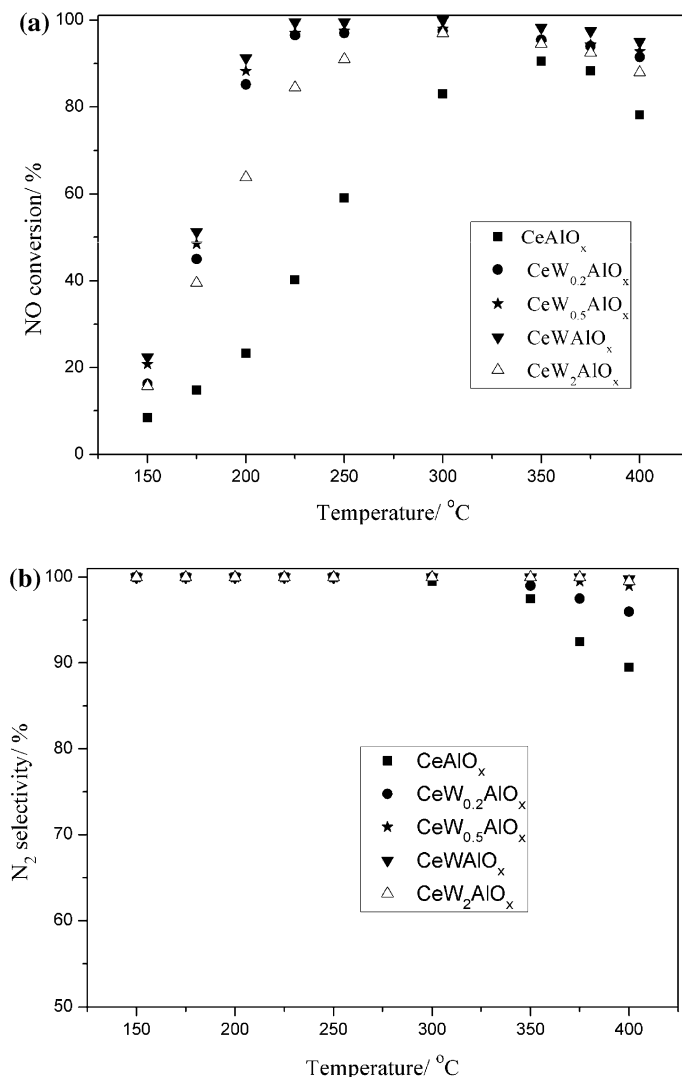


**Fig. 1** a NH<sub>3</sub>-SCR catalytic activity b N<sub>2</sub> selectivity over CeAlO<sub>x</sub> and Ce–W–AlO<sub>x</sub> catalysts under GHSV of 30,000 h<sup>-1</sup>

was detected in the all catalysts. As the W doped molar ratio increased from 0.2 to 2.0, almost no changes occurred in the intensities of the CeO<sub>2</sub> peaks. Combining the XRD and NH<sub>3</sub>-SCR catalytic activity evaluation results, there must be some synergistic effect among Ce, W and Al oxides in the W modified CeAlO<sub>x</sub> catalyst.

### BET

The BET results of the CeAlO<sub>x</sub> and W modified CeAlO<sub>x</sub> catalysts are summarized in Table 1. It can be seen that the introduction of W into the CeAlO<sub>x</sub> catalyst could

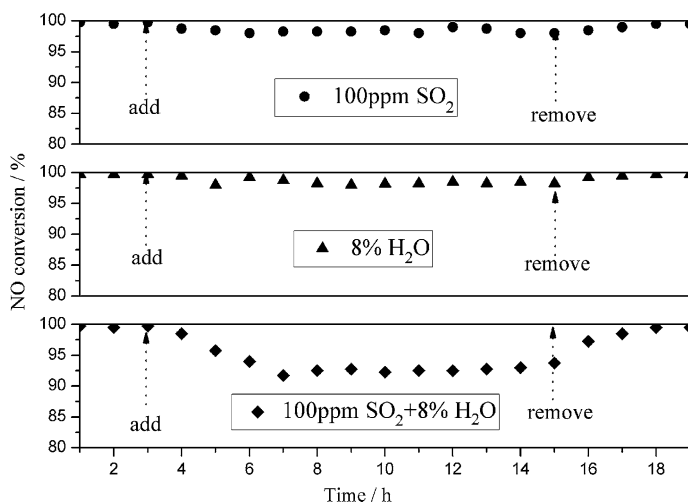


**Fig. 2**  $\text{NH}_3$ -SCR activity over  $\text{CeWAlO}_x$  catalyst in the presence of 100 ppm  $\text{SO}_2$  or/and 8 %  $\text{H}_2\text{O}$  under GHSV of  $30,000 \text{ h}^{-1}$

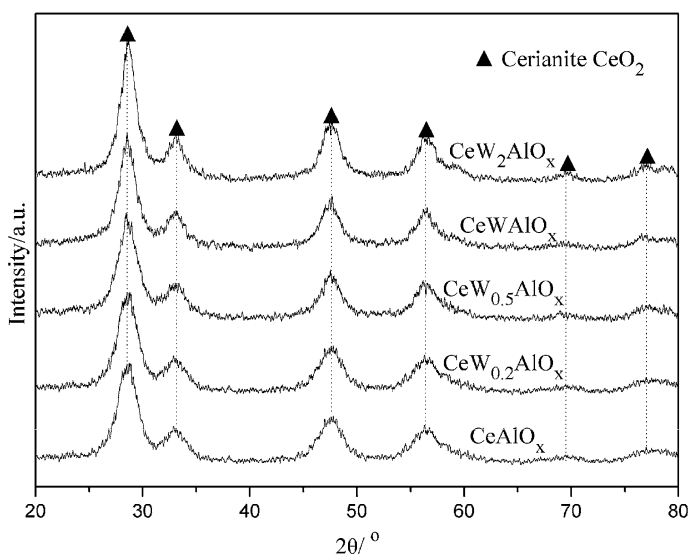


**Fig. 3** XRD patterns of the  $\text{CeAlO}_x$  and  $\text{Ce-W-AlO}_x$  catalysts. **a**  $\text{CeAlO}_x$ , **b**  $\text{CeW}_{0.2}\text{AlO}_x$ , **c**  $\text{CeW}_{0.5}\text{AlO}_x$ , **d**  $\text{CeWAlO}_x$ , **e**  $\text{CeW}_2\text{AlO}_x$

lead the surface area lower at different degrees, while the total pore volume and the average pore diameter were enlarged at different extents. The surface area, pore volume and average pore diameter of  $\text{CeAlO}_x$  were  $158 \text{ m}^2/\text{g}$ ,  $0.18 \text{ cm}^3/\text{g}$  and  $3.7 \text{ nm}$ . When the W/Al molar ratio reached 1.0, the surface area of the  $\text{CeWAlO}_x$  catalyst dropped to  $108 \text{ m}^2/\text{g}$ , while the pore volume and average pore diameter

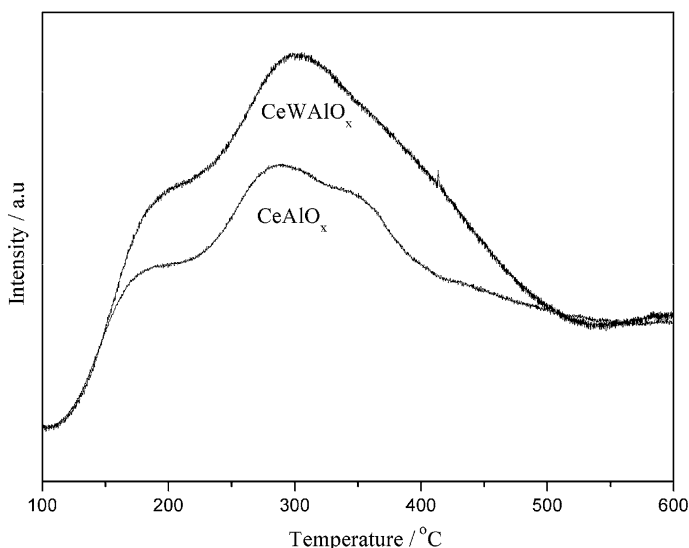
**Table 1** Physical properties of the Ce–W–AlO<sub>x</sub> catalysts

Sample	BET surface area (m <sup>2</sup> /g)	Pore volume (cm <sup>3</sup> /g)	Average pore diameter (nm)
CeAlO <sub>x</sub>	158	0.18	3.7
CeW <sub>0.2</sub> AlO <sub>x</sub>	118	0.21	6.5
CeW <sub>0.5</sub> AlO <sub>x</sub>	113	0.23	8.5
CeWAlO <sub>x</sub>	108	0.28	9.4
CeW <sub>2</sub> AlO <sub>x</sub>	103	0.22	5.9

increased to the maximum 0.28 cm<sup>3</sup>/g and 9.4 nm, respectively. However, the surface area, pore volume and average pore diameter decrease gradually with further doping tungsten on the CeAlO<sub>x</sub> catalyst. The above results indicated that the BET parameter was not the key factor to influence the NH<sub>3</sub>-SCR activity.

### NH<sub>3</sub>-TPD

The amount of acid sites on the catalyst surface is crucial to the NH<sub>3</sub>-SCR reaction, which can be characterized by the NH<sub>3</sub>-TPD. The corresponding NH<sub>3</sub>-TPD curves of the CeAlO<sub>x</sub> and CeWAlO<sub>x</sub> catalysts are shown in Fig. 4. As can be seen from the figure, the desorption curve of the CeAlO<sub>x</sub> catalyst possessed three desorption peaks. The first peak at 184 °C can be assigned to the weakly bonded NH<sub>3</sub>, the peaks at 287 and 355 °C can be attributed to the strongly adsorbed NH<sub>3</sub>. The total acidity of the CeAlO<sub>x</sub> catalyst was about 554 μmol/g. For the CeWAlO<sub>x</sub> catalyst, the strongly adsorbed NH<sub>3</sub> peak at 298 °C disappeared and the total acidity increased to around 763 μmol/g, which suggested that the surface acidity of the

**Fig. 4** NH<sub>3</sub>-TPD profiles of the CeAlO<sub>x</sub> and CeWAlO<sub>x</sub> catalysts

CeWAIO<sub>x</sub> catalyst was strengthened by doping with W. Combining the NH<sub>3</sub>-SCR activity results with the NH<sub>3</sub>-TPD curves indicates that the increase of the surface acidity was a key factor to enhance the catalytic activity.

### H<sub>2</sub>-TPR

Apart from the surface acidity of the catalyst, the reducibility of the catalyst also plays an important role during the NH<sub>3</sub>-SCR reaction. The redox activity changes of the catalysts were investigated by H<sub>2</sub>-TPR and the corresponding profiles of the CeAlO<sub>x</sub> and CeWAIO<sub>x</sub> are displayed in Fig. 5. It can be seen from the figure that the CeAlO<sub>x</sub> profile showed one broad reduction peak from 300 to 600 °C due to the reduction of surface Ce<sup>4+</sup> to Ce<sup>3+</sup> [8]. For the CeWAIO<sub>x</sub> catalyst, the reduction peak shifted to around 526 °C, and the area of the reduction peak became larger, which indicates that the redox activity was enhanced. The above result suggested that the mobility of the surface oxygen was enhanced after introduction of W, which was beneficial to the NH<sub>3</sub>-SCR reaction.

### XPS

It was reported that higher Ce<sup>3+</sup>/Ce<sup>4+</sup> molar ratio on the catalyst surface is helpful to the NH<sub>3</sub>-SCR reaction [9]. The XPS results of the Ce on the CeAlO<sub>x</sub> and CeWAIO<sub>x</sub> surfaces are depicted in Fig. 6. The Ce 3d peaks were fitted by searching for the optimum combination of Gaussian bands. The sub-bands labeled u' and v' represent the 3d<sup>10</sup>4f<sup>1</sup> initial electronic state corresponding to Ce<sup>3+</sup>, and the sub-bands labeled u, u'', u''', v, v'', and v''' represent the 3d<sup>10</sup>4f<sup>0</sup> state of Ce<sup>4+</sup>. The Ce<sup>3+</sup>

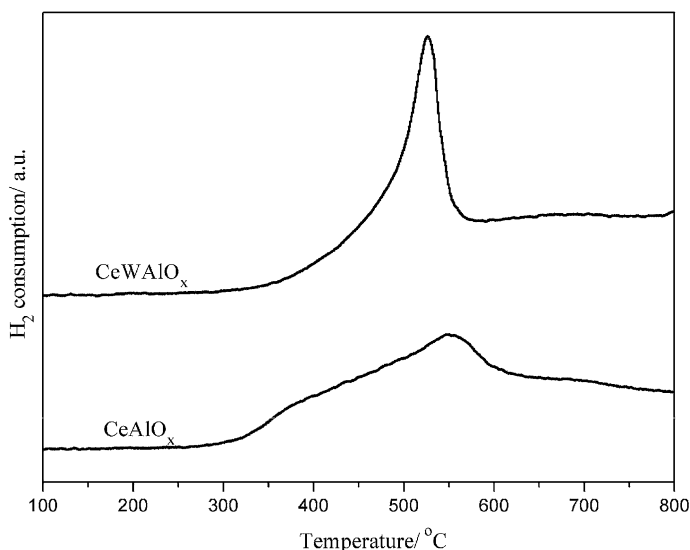


**Fig. 5** H<sub>2</sub>-TPR profiles of the CeAlO<sub>x</sub> and CeWAIO<sub>x</sub> catalysts



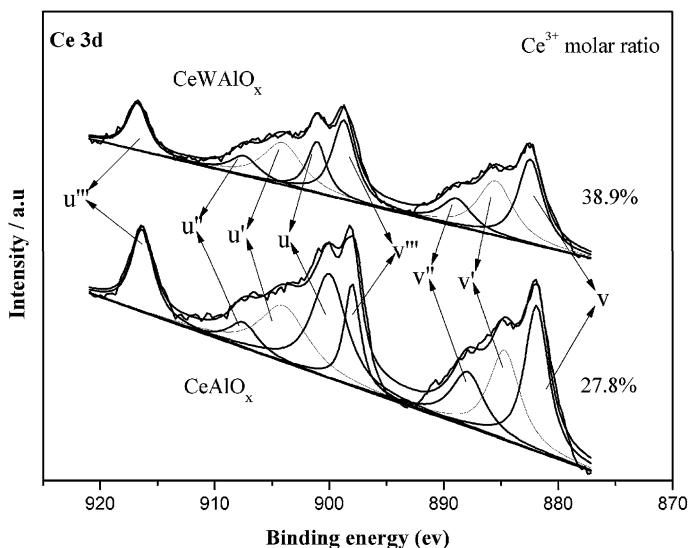


**Fig. 6** XPS profiles of the  $\text{CeAlO}_x$  and  $\text{CeWAlO}_x$  catalysts

ratio, calculated by  $\text{Ce}^{3+}/(\text{Ce}^{3+} + \text{Ce}^{4+})$  of  $\text{CeWAlO}_x$  (38.9 %) was significantly higher than that of  $\text{CeAlO}_x$  (27.8 %), indicating the presence of more surface oxygen vacancies on  $\text{CeWAlO}_x$ . The above result was consistent with the Shan's report [9].

### *In situ DRIFTS*

In order to examine the changes of  $\text{NH}_3$  adsorbed on the surface of the  $\text{CeAlO}_x$  and  $\text{CeWAlO}_x$  catalysts, the *in situ* DRIFTS of  $\text{NH}_3$  adsorption result over  $\text{CeAlO}_x$  and  $\text{CeWAlO}_x$  catalysts at 200 °C are presented in Fig. 7. As shown in the figure, the band at  $1270 \text{ cm}^{-1}$  is assigned to the symmetric and asymmetric deformation vibration of  $\text{NH}_3$  adsorbed on Lewis acid site [10]; the band at  $1502 \text{ cm}^{-1}$  can be attributed to ionic  $\text{NH}_4^+$  species on Brønsted acid site [11]. In the meanwhile, the band at  $1148 \text{ cm}^{-1}$  is due to the scissoring vibration mode of  $\text{NH}_2$  species [12]; the bands at  $3275$  and  $3380 \text{ cm}^{-1}$  are attributed to N–H stretching vibration modes [13]; some negative bands at  $3632$  and  $3792 \text{ cm}^{-1}$  belong to the surface O–H stretching were also detected [14, 15]. After the addition of W, the band assigned to the scissoring vibration mode of  $\text{NH}_2$  species disappeared obviously. However, the band at  $1284 \text{ cm}^{-1}$  assigned to the Lewis acid site and the bands at  $1178$  and  $1425 \text{ cm}^{-1}$  corresponding to the Brønsted acid site were much stronger than that on the  $\text{CeAlO}_x$  catalyst [16–18]. In the meantime, much stronger bands at  $3178$ ,  $3266$  and  $3366 \text{ cm}^{-1}$  attributed to N–H stretching vibration modes were also detected on the  $\text{CeWAlO}_x$  catalyst [13]. The above analysis indicated that both the Lewis and Brønsted acid strength were increased by the introduction of W, according to some previous studies, the increased Lewis acid are mainly composed of unsaturated  $\text{W}^{n+}$  cations [19], while the increased Brønsted acid are mainly composed of W–OH site

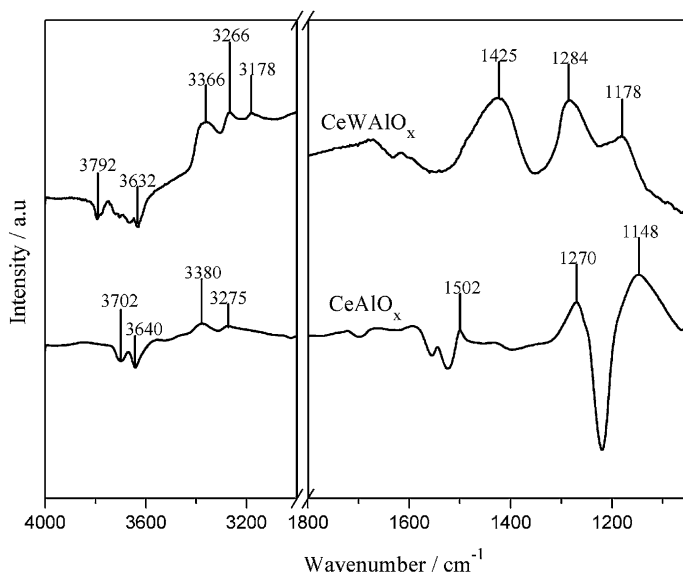


**Fig. 7** In situ DRIFTS spectra of  $\text{NH}_3$  adsorption on the  $\text{CeAlO}_x$  and  $\text{CeWAlO}_x$  catalysts at  $200\text{ }^\circ\text{C}$

arising from partially hydrated tungsten species, such as  $\text{W}=\text{O}$ ,  $\text{W}-\text{O}-\text{W}$  and  $\text{Ce}-\text{W}-\text{O}$  [20–22]. The above results were also consistent with the  $\text{NH}_3$ -TPD result.

## Conclusions

A series of tungsten modified  $\text{CeAlO}_x$  catalysts were prepared by the homogeneous co-precipitation method and used for the selective catalytic reduction of  $\text{NO}$  with  $\text{NH}_3$ . It is concluded that the  $\text{NH}_3$ -SCR catalytic activity of the  $\text{CeAlO}_x$  could be markedly improved by the substitution with  $\text{W}$ . The  $\text{CeWAlO}_x$  catalyst also showed high resistant to the  $\text{SO}_2$  and  $\text{H}_2\text{O}$  poisoning in the tested condition. As can be seen from the characterization results of the BET, XRD,  $\text{NH}_3$ -TPD,  $\text{H}_2$ -TPR, XPS and in situ DRIFTS, the pore volume and the average pore diameter of  $\text{CeAlO}_x$  can be increased by addition of  $\text{W}$ . The acidity, redox property and  $\text{Ce}^{3+}/\text{Ce}^{4+}$  molar ratio were also enhanced by modification with  $\text{W}$ . The higher acidity, better redox ability, stronger adsorption capability to the  $\text{NH}_3$  and much more oxygen vacancies on the catalyst surface played important roles for the  $\text{CeWAlO}_x$  catalyst to achieve high  $\text{NH}_3$ -SCR performance.

## References

1. Qi G, Yang RT (2003) *Appl Catal B Environ* 44(3):217–225
2. Zhang D, Zhang L, Shi L et al (2013) *Nanoscale* 5(3):1127–1136
3. Li X, Li Y (2014) *React Kinet Mech Cat* 112(1):27–36

4. Shan W, Liu F, He H et al (2011) *Chem Commun* 47(28):8046–8048
5. Shen Y, Zhu S, Qiu T et al (2009) *Catal Commun* 11(1):20–23
6. Guo R, Zhou Y, Pan W et al (2013) *J Ind Eng Chem* 19(6):2022–2025
7. Li X, Li Y (2014) *J Mol Catal A: Chem* 386:69–77
8. Murugan B, Ramaswamy AV (2008) *J Phys Chem C* 112(51):20429–20442
9. Shan W, Liu F, He H et al (2012) *Appl Catal B Environ* 115:100–106
10. Stoilova D, Cheshkova K (1998) Nickolov R. *React Kinet Catal L* 65(2):265–270
11. Oktar N, Mitome J, Holmgren EM et al (2006) *J Mol Catal A: Chem* 259(1):171–182
12. Wang C, Yang S, Chang H et al (2013) *J Mol Catal A: Chem* 376:13–21
13. Busca G, Larrubia MA, Arrighi L et al (2005) *Catal Today* 107:139–148
14. Topsøe NY, Anstrom M, Dumesic JA (2001) *Catal Lett* 76(1–2):11–20
15. Huang SJ, Walters AB, Vannice MA (2000) *Appl Catal B Environ* 26(2):101–118
16. Sultana A, Nanba T, Haneda M et al (2010) *Appl Catal B Environ* 101(1):61–67
17. Liu F, He H (2010) *Catal Today* 153(3):70–76
18. Nicosia D, Czekaj I, Kröcher O (2008) *Appl Catal B Environ* 77(3):228–236
19. Busca G, Lietti L, Ramis G et al (1998) *Appl Catal B Environ* 18(1):1–36
20. Alemany LJ, Lietti L, Ferlazzo N et al (1995) *J Catal* 155(1):117–130
21. Mamede AS, Payen E, Grange P et al (2004) *J Catal* 223(1):1–12
22. Kobayashi M, Miyoshi K (2007) *Appl Catal B Environ* 72(3):253–261